

D. Heitz · P. Héas · V. Navaza · J. Carlier · E. Mémin

## Spatio-temporal correlation-variational approach for robust optical flow estimation

**Abstract** We present in this paper a novel collaborative scheme dedicated to the measurement of velocity in fluid experimental flows through image sequences. The proposed technique combine the robustness of correlation techniques with the high density of global variational methods. It can be considered either as a reinforcement of fluid dedicated optical-flow methods towards robustness, or as an enhancement of correlation approaches towards dense information. This results in a technique that is robust under noise and outliers, while providing a dense motion field. The method was applied on synthetic images and on real experiments in turbulent flows carried out to allow a thorough comparison with a state of the art optical-flow and PIV methods.

**Keywords** Fluid motion measurement · Optical-flow · PIV · Correlation · Variational approach

### 1 Introduction

Particule Image Velocimetry (PIV) is now a widely used measurement technique in the investigation of turbulent engineering flows. Its proven ability to capture time series of instantaneous, two or three component velocity data over a planar field allows the fluid dynamist to analyse the structure of the flow. PIV allows us to observe fluid dynamics phenomena previously extremely difficult to detect with point measurement like hot wire anemometry (HWA) for instance.

PIV techniques are based on a spatio-temporal cross-correlation submitted to a consistency assumption of the flow within a local interrogation window. The interrogation windows generally contain several particles with different mo-

tions. Considering a unique motion vector for all these particles may lead on one hand to poor local motion representation. On the other hand, the extraction of the most probable displacement in the interrogation area offers high robustness under noise. Indeed, this approach introduces a low-pass filtering effect.

Recent studies have outlined the possibility of treating the flow images as continuous system of flow structures, instead of a system of quasi-random points. Developed by the vision community, new techniques computing the optical flow, have been applied with success on particule images to investigate fluid flows (Ruhnau *et al.*, 2005; Corpetti *et al.*, 2006). Based on the formulation introduced by Horn & Schunck (1981), these variational approaches provide a *dense* motion fields (i.e. one vector per pixel). Classified into *global* approaches (Bruhn *et al.*, 2005), these techniques consist in estimating a vectorial function by minimizing a global objective functional composed of two terms; the data model and a regularization term. The former is an adequacy term between the unknown motion function and the data. It generally relies on a brightness consistency assumption. Similarly to correlation techniques, this assumption states that a given point keeps its intensity along its trajectory. The latter promotes a global smoothness of the motion field over the image. The use of a regularization term as a smoothing technique is a typical way to overcome the aperture problem (Bertero *et al.*, 1988). This ill-posedness problem manifests itself in the nonuniqueness of the solution provided by the data term. Another way to tackle this problem consists in considering with the data term a local spatial (Lucas & Kanade, 1981) or spatiotemporal (Bigün & Granlund, 1988) constancy assumptions on the optic flow field. As a consequence these *local* methods provide robust estimation but sparse flow fields, compare to *global* approaches which yield dense fields and are sensitive to noise. Bruhn *et al.* (2005) proposed a combined local-global method which has the robustness of local methods with the density of global approaches. Unfortunately, this technique, not specifically suited for fluid flow, was not tested on particule images.

Corpetti *et al.* (2002, 2006) proposed a novel optical flow technique dedicated to image sequences depicting fluid flow

D. Heitz - V. Navaza - J. Carlier  
Cemagref, 17, avenue de Cucillé, CS64427, F-35044 Rennes Cedex - France  
Tel.: +33-2-23482170  
Fax: +33-2-23482115  
E-mail: dominique.heitz@cemagref.fr

P. Héas - E. Mémin  
IRISA/INRIA, Campus Universitaire de Beaulieu, F-35042 Rennes Cedex - France

phenomena. This specialized optical-flow estimator relies on an adaptation of the functional observation and regularization terms. Instead of sticking to the intensity conservation assumption, the data-model considered relies on the continuity equation as a more physically-grounded alternative. As for the regularization, a second-order regularizer is used to preserve completely the divergence and vorticity structures of the flows. Using a div-curl formalism, a second-order regularizer is introduced to capture the divergence and vorticity of the unknown flow.

To handle large displacements the data term is generally used in an integrated way, linearized around a previous estimate and embedded within a multiresolution coarse-to-fine scheme (Bergen *et al.*, 1992). Standard multiresolution approach consists in deriving the original frame into a pyramid of images, by successive low-pass filtering (Gaussian smoothing) and regular subsampling by a factor of two in each direction. The created pyramid structure then allows multiscale motion estimation by incremental procedure. Low resolution components are estimated at coarsest level and then refined step by step: at a resolution level, an increment velocity field is estimated around the projection (by duplication or interpolation) of the final estimate at previous resolution level. In general the procedure of filtering and subsampling leads to a loss of information. The proper choice of filter depends not only on the sampling theorem but also on the distribution of the energy of the image spectrum.

In the case of particle images of turbulent fluid flows, small particles with large velocities, can be smoothed out by the multiresolution procedure. Therefore, due to this loss of information, the optical flow approach will not extract the true velocity. Indeed, within the energy minimization framework, finding the global minimum of the cost function will be tricky if the initialization is wrong or far from the minimum. In case of robust estimation the problem will be increased since robust estimation leads most of the time to a global nonlinear minimization in presence of numerous local minima. In region with a low density of particles and a certain amount of noise in the image or with a poor range of grey level, the multiresolution procedure will enhance the impact of the noise on the result. Indeed, at the coarsest level, the subsampling process keeps statistically more noise than particle information when there is poor particle density and noise in the original image.

In this paper, we propose to design a novel approach that combine the robustness of correlation techniques with the high density of global variational methods. This results in a technique that is robust under noise and outliers, while providing a dense motion field.

This article is organized as follows. In a first section, we present the fluid dedicated global approaches. Then, in a second section, we present the collaborative approach. In a last part, results from synthetic images based on a DNS of 2D turbulence, and real images in the wake of a circular cylinder, are presented and analysed. We provide some elements of comparison of our method with standard optical flow techniques.

## 2 Multiscale motion estimation

### 2.1 Classical method

The apparent motion, perceived through variations of image intensity  $I$  is called *optical flow* in the computer vision community. All optical flow estimation methods rely on the temporal conservation of some invariants. The most common ones are photometric ones which can easily be extracted and may lead to dense measurements. In the case of PIV imagery for bi-dimensional flows visualization, the gray level constancy assumption can be assumed. Let us denote by  $\mathbf{s}$  the spatial coordinates  $(x, y)$  and by  $\mathbf{u}(\mathbf{s})$  the apparent motion field at this point and at a given time  $t$ . This invariant leads to an integrated non-linear formulation called the Displaced Frame Difference (DFD) equation  $I(\mathbf{s} + \mathbf{u}(\mathbf{s}), t + 1) = I(\mathbf{s}, t)$ , or at time  $t$ , to a linear differential formulation called the Optical Flow Constraint (OFC) equation  $\mathbf{u}(\mathbf{s}) \cdot \nabla I(\mathbf{s}) + I_t(\mathbf{s}) = 0$ .

These two formulations can not be used alone, as they provide only one equation for two unknowns at each spatio-temporal location  $(\mathbf{s}, t)$ . This is the well known *aperture problem* where the so called *normal flow* is estimated while the tangential velocity component remains undetermined. In order to remove this ambiguity and robustify the estimation, one must rely on other assumptions. The main used assumption is spatial *local coherence*. This assumption may be expressed as a regularity prior on velocity field spatial smoothness.

A very common approach used with PIV imagery is correlation-based matching, which corresponds to the DFD constraint associated to a locally constant field within a neighborhoods  $W(\mathbf{s})$ . Thus, using a discrete space of vectors  $\{\mathbf{w}\}$ , the velocity  $\mathbf{u}$  at point  $\mathbf{s}$  is obtained as

$$\mathbf{u}(\mathbf{s}) = \arg \min_{\mathbf{w}} \sum_{\mathbf{r} \in W(\mathbf{s})} \mathcal{C}(I(\mathbf{r} + \mathbf{w}, t + 1), I(\mathbf{s}, t)) \quad (1)$$

where  $\mathcal{C}(\cdot)$  denotes a dissimilarity function. On the one hand, these approaches suffer from several deficiencies : traceable features must be sufficiently contrasted and must persist over time on consecutive images. Furthermore, the estimation prone to erroneous spatial variability, which can be reduced with the use of filters. On the other hand, these techniques constitute very fast methods and are generally locally very robust to noise. These techniques are based on disjoint local estimation, and thus produce sparse vector fields estimated locally and independently.

### 2.2 Fluid dedicated optical flow method

Alternate approaches are optical flow estimators derived in the framework of Horn & Schunck (1981) methodology. They have the great advantage of producing dense vector fields. They are based on the minimization of an energy function  $J = J_d + J_r$  composed of two terms. The first term  $J_d$  is called the data term and implements the OFC equation

$$J_d(\mathbf{u}, I) = \int_{\Omega} \phi[\nabla I(\mathbf{s}) \cdot \mathbf{u}(\mathbf{s}) + \frac{\partial I(\mathbf{s})}{\partial t}] ds. \quad (2)$$

The penalty function  $\phi$  is usually the  $L_2$  norm but it may be changed to a robust function attenuating the effect of data that deviate significantly from the OFC (Black & Anandan, 1996). The second term  $J_r$  is called the regularization term. It is usually a standard first-order spatial smoothness term

$J_r(\mathbf{u}) = \alpha \int_{\Omega} \phi(\|\nabla \mathbf{u}\|) ds$ , where  $\alpha > 0$  is a parameter controlling the balance between the smoothness and the global adequacy to the brightness constancy assumption. Function  $\phi$  may be the quadratic penalty if the searched solution is smooth everywhere or a robust norm function if one wants to handle implicitly the spatial discontinuities of the field (Black & Anandan, 1996). However in the case of fluid flows, it can be demonstrated that a first order regularization is not adapted as it favors the estimation of velocity fields with low vorticity. A second order regularization can advantageously be considered as proposed in (Suter, 1994) :

$$J_r(\mathbf{u}) = \alpha \int_{\Omega} \phi(\|\nabla \xi(\mathbf{s})\|^2 + \|\nabla \zeta(\mathbf{s})\|^2) ds, \quad (3)$$

where  $\xi = \text{curl} \mathbf{u} = \frac{\partial u}{\partial y} - \frac{\partial v}{\partial x}$  and  $\zeta = \text{div} \mathbf{u} = \frac{\partial u}{\partial x} + \frac{\partial v}{\partial y}$  stand for the vorticity and divergence of the apparent velocity  $\mathbf{u} = (u, v)^T$ . Note that in the case of bi-dimensional incompressible flows, divergence of the apparent motion is equal to zero. To circumvent the difficulty of implementing second order smoothness constraint, this regularization term can be simplified in a computational point of view in two interleaved first-order div-curl regularizations based on an auxiliary variable  $\xi_1$  and  $\zeta_1$  approximating the vorticity and the divergence of the flow (Corpetti *et al.*, 2002, 2006). Thus we have :

$$J_r(\mathbf{u}) = \alpha \int_{\Omega} \phi[(\xi(\mathbf{s}) - \xi_1)^2 + \beta \|\nabla \xi_1\|^2] ds \quad (4)$$

$$+ \alpha \int_{\Omega} \phi[(\zeta(\mathbf{s}) - \zeta_1)^2 + \beta \|\nabla \zeta_1\|^2] ds, \quad (5)$$

where  $\beta$  is a positive regularization parameter.

### 2.3 Multiresolution approach

However, one major problem with optical flow estimators is large displacement estimation. The intensity function must be locally sufficiently close to a linear function. Since the larger the displacement the more narrow the linearity domain is, large displacements can not be recovered directly. A common way to overcome this limitation is to create a image pyramid, constructed by successive low-pass filtering and down sampling of the original images. In this framework, principal components of displacements are first estimated at coarse resolution where motion amplitude should be sufficiently reduced in order to satisfy the linearity requirement. Incremental displacement are then estimated while going down the pyramid, and the solution is refined (Bergen *et al.*, 1992). However, since the multiresolution schemes estimates principal component displacements only at coarse resolutions where small structures are rubbed out, this approach

enables the characterization of large displacements of small structures only in the case when their motion are close enough to the principal component's one. Another disadvantage characterizing the method is the additional noise incorporation due to the calculation of motion-compensated images at each resolution by the use of interpolation methods.

### 3 Collaborative correlation-optical flow scheme

To overcome the multiresolution limitations, we propose an alternative approach relying on a unique representation of the full resolution image. Thus, the proposed method tackles the non-linear estimation problem without making successive approximations in the calculation of interpolated images nor restricting itself to the characterization of large displacements of sufficiently large structures. The proposed method takes advantage of the non-linear formulation of the motion estimation problem within a differential framework appropriated for globalized local smoothings. More explicitly, large displacements of both, fine or large structures, can be recovered by correlation-based methods for sufficiently contrasted and persisting image regions. Thus, the idea of the method is to replace the coarse estimates of the multiresolution scheme by a dense large scale displacement estimate derived from a collection of correlation-based vectors  $\mathbf{u}_c$  obtained by Eq.1.

The displacement field  $\mathbf{d}$  is decomposed into a large scale  $\bar{\mathbf{u}}$  and a small scale  $\mathbf{u}'$  displacement field :  $\mathbf{d} = \bar{\mathbf{u}} + \mathbf{u}'$ . This decomposition is used to define a new functional for estimation of variables  $\bar{\mathbf{u}}$  and  $\mathbf{u}'$

$$J(\bar{\mathbf{u}}, \mathbf{u}') = J_d(I, \bar{\mathbf{u}} + \mathbf{u}') + J_r(\bar{\mathbf{u}} + \mathbf{u}') + J_c(\bar{\mathbf{u}}, \mathbf{u}_c), \quad (6)$$

where  $J_c(\cdot)$  is the energy function constraining large scale estimated displacements  $\bar{\mathbf{u}}$  to be close to a sparse correlation-based vector field  $\mathbf{u}_c$ . Thus, functional  $J_c(\cdot)$  is defined as a quadratic distance between the solution and a collection of correlation-based vectors  $\mathbf{u}_c^i = (u^i, v^i)$  located at the point  $\mathbf{s}^i = (x^i, y^i)$  and influencing their neighborhood according to a shifted bi-dimensional Gaussian law  $\mathcal{N}^i(\mathbf{s}^i - \mathbf{s})$  of variance  $\sigma$

$$J_c(\bar{\mathbf{u}}, \mathbf{u}_c) = \gamma \int_{\Omega} \sum_{i=1}^K g^i \mathcal{N}^i(\mathbf{s}^i - \mathbf{s}) \|\mathbf{u}_c^i - \mathbf{u}(\mathbf{s})\|^2 ds. \quad (7)$$

In the previous expression,  $g^i$  and  $\gamma$  denote respectively confidence factors and the functional weighting factor.

Two different collaborative schemes were evaluated in the following. Collaborative 1 scheme, involves two steps. The minimization problem is conducted sequentially. In a first step, large scale displacements  $\bar{\mathbf{u}}$  are estimated while the variable  $\mathbf{u}'$  is fixed to zero. Thus, Eq.6 reduces to  $J(\bar{\mathbf{u}}) = J_d(I, \bar{\mathbf{u}}) + J_r(\bar{\mathbf{u}}) + J_c(\bar{\mathbf{u}}, \mathbf{u}_c)$ . Here, an analogous version of the alternate multigrid minimization scheme proposed in Corpetti *et al.* (2002); Mémin & Pérez. (2002) is derived, the only difference being in the Gauss-Seidel solver for variable

$\bar{\mathbf{u}}$  estimation. Once the minimum has been reached, a second refinement step is launched : the small scales displacement increments  $\mathbf{u}'$  are estimated while the variable  $\bar{\mathbf{u}}$  is frozen. More explicitly,  $\bar{\mathbf{u}}$  is used to derive a motion-compensated expression of the data model  $J_d(\cdot)$  and to express the div-curl regularizer in terms of the displacement increment  $\mathbf{d} - \bar{\mathbf{u}}$ . As functional  $J_c(\cdot)$  does not depend on the small scale displacement increments, it is removed. Consequently, for this refinement step, we recover the fluid-dedicated estimator defined in Corpetti *et al.* (2002, 2006). Collaborative 2 scheme involves one step.  $\bar{\mathbf{u}}$  and  $\mathbf{u}'$  are estimated at the same time with eq. 6.

## 4 Numerical evaluation

### 4.1 Synthetic image sequence

To evaluate the performance of the collaborative approach compare to state of the art optical-flow and correlation approaches, a synthetic particle image sequence was generated based on the direct numerical simulation (DNS) of 2D turbulent flow (Carlier & Wieneke, 2005). The present flow contains typical difficulties for image based measurements techniques, like high velocity gradients and large dynamic range. The Reynolds number based on a characteristic length scale was equal to 30 000. Figure 1 presents the whole flow domain and the region considered for a thorough comparison.

The image sequence was generated with a home-made particle image generator involving comparable methods than those developed for the EUROPIV Synthetic Image Generator (Lecordier & Westerweel, 2003). A velocity-vorticity formulation of the Navier-Stokes equations was adopted for the DNS. The vorticity equation was solved in Fourier space using dealiased Fourier expansions in two directions with periodic boundary conditions. The time integration was third-order/three steps with a Runge-Kutta scheme. The code is called pseudo-spectral. The coordinates of each particles were calculated in the physical space inside the vorticity equation computation using the Runge-Kutta scheme of the DNS in order to use the intermediate velocity components. However, a bicubic interpolation of the velocity field was applied since the particles were not supposed to be located at the nodes of the grid.

In the present evaluation the image pair considered led to a maximum particle image displacement up to 6 px. This particle image displacement was globally optimum to minimize the RMS error provided by the optical flow technique. This relatively small maximum displacement necessitates a multiresolution pyramid with only two levels. However, the addition of noise in the image pairs enables to put optical-flow technique, involving multiresolution scheme, on the wrong track.

In order to provide more realistic conditions the signal to noise ratio was increased, simulating a reduction of the power of the virtual laser. The noise was quantified with peak signal-to-noise ratio (PSNR) which is the ratio between

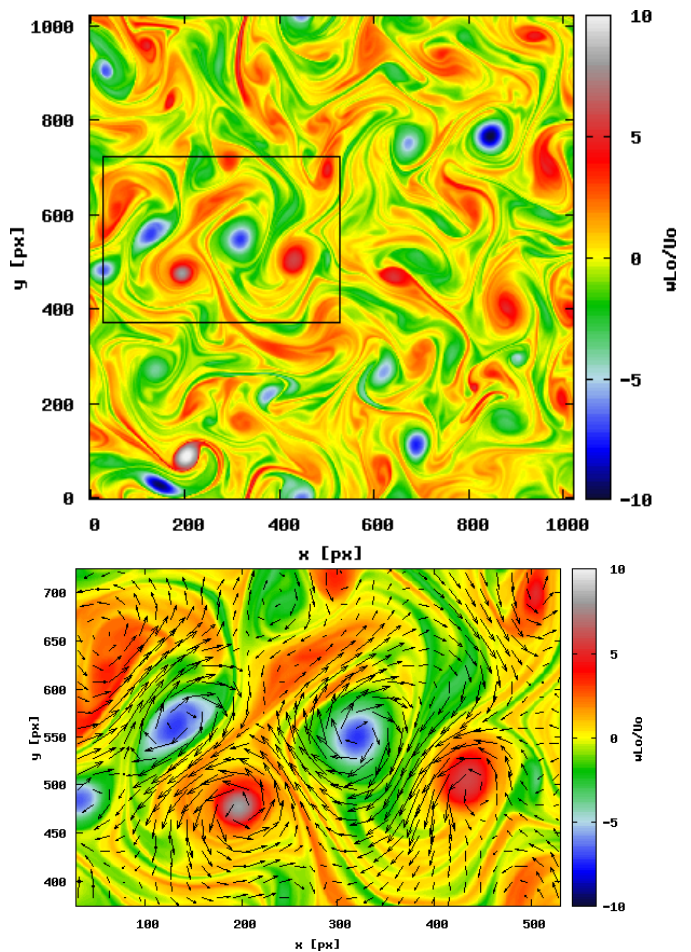


**Fig. 1** 2D turbulence test case - Color map of the normalized vorticity with superposed velocity field.

the maximum possible power of a signal and the power of corrupting noise that affects the fidelity of its representation. Because many signals have a very wide dynamic range, PSNR is usually expressed in terms of the logarithmic decibel scale. The PSNR is most commonly used as a measure of quality of reconstruction in image compression. The PSNR is defined as:

$$PSNR = 10 \log_{10} \left( \frac{d^2}{MSE} \right)$$

where  $d$  is the dynamic of the grey level of the signal, here the particles. For an image where the particles are represented over 8 bits  $d = 2^8 - 1 = 255$ . MSE is the mean squared error, which for two  $m \times n$  images  $I_o$  and  $I_r$  where one of the images is considered a noisy approximation of the other, is defined as:

$$MSE = \frac{1}{mn} \sum_{i=0}^{m-1} \sum_{j=0}^{n-1} \|I_o(i, j) - I_r(i, j)\|^2$$

Typical PSNR values for images of good quality lie between 30 and 40 dB.

To estimate correlation-based velocity fields, the commercial software DaVis 6.2 from LaVision was used. A multipass algorithm with a final interrogation window size of  $16 \times 16 \text{ px}^2$  and 50% overlapping was applied. Image deformation and round gaussian weighing function were used. Spurious velocities were identified with median filter and replaced by the median. The vector fields obtained with this correlation technique were used in the collaborative approach.

#### 4.2 Multiresolution limitations

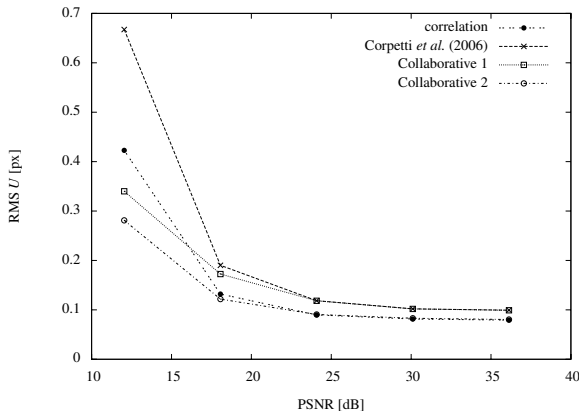


Fig. 2 RMS of the error of the horizontal velocity component.

The RMS errors of the different approaches (correlation, optical flow and collaborative) are shown in figure 2. For all methods the RMS error was increasing with decreasing values of PSNR (increasing noise). Whatever the value of PSNR, the highest error appeared for optical-flow technique from Corpetti *et al.* (2006). For  $\text{PSNR} \geq 30 \text{ dB}$ , i.e. for images of good quality, this slight larger error is due to the numerical scheme used to mimic second order regularization (Heitz *et al.*, 2006). For  $\text{PSNR} < 30 \text{ dB}$ , image noise influence in the estimated velocities was observed. For  $\text{PSNR} = 12 \text{ dB}$ , i.e. for very poor image quality, the large error was mainly explained by the inaccurate estimation of the large displacements. Figure 3 clearly illustrates this behaviour. It shows the vector field of the exact solution for region of large displacements (for  $\|\mathbf{u}\|/\|\mathbf{u}\|_{\max} > 30\%$ , i.e. for displacements larger than 2 pixels) and the map of color of the deviation of optical-flow from the exact velocity modulus. For regions of large velocities the deviation from the exact solution ranged between 40 % and 100 %. The addition of noise in the images combined with the down sampling of the multiresolution scheme smoothed out the particle informations. With smaller particles and/or larger displacements, this effect would have been enhanced and already observed for larger values of PSNR.

The inaccurate estimation of the large displacements led to a poor extraction of the dynamic especially at large scales. This phenomenon was observed in figure 4 by considering

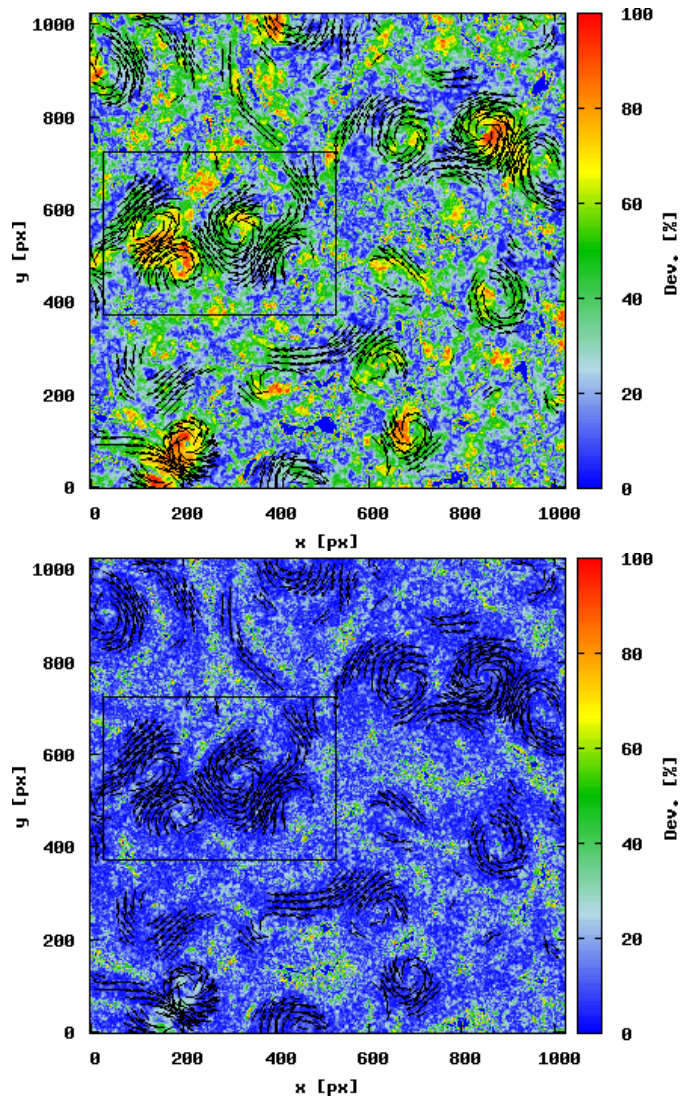


Fig. 3 Map of color of the deviation of Corpetti *et al.* (2006) from the exact velocity modulus – Vector field of the exact solution for  $\|\mathbf{u}\|/\|\mathbf{u}\|_{\max} > 30\%$ . Top:  $\text{PSNR} = 12 \text{ dB}$ ; Bottom,  $\text{PSNR} = 18 \text{ dB}$ .

compensated spectra. For  $\text{PSNR} = 12 \text{ dB}$ , the optical-flow approach completely failed to estimate the dynamic in the flow. For  $\text{PSNR} = 18 \text{ dB}$ , the large displacements were more precisely measured. As indicated in figure 3, the deviation from the exact solution was lower than 5%. However, figure 4 shows for  $\text{PSNR} = 18 \text{ dB}$  that, despite the accurate determination of large velocities, some discrepancies remained in the description of the largest scales. This behaviour at large scale explained the lack of performance of the scheme proposed by Corpetti *et al.* (2006) compared to correlation technique, see figure 2. As discussed above the accurate optical flow scheme proposed by Yuan *et al.* (2007), using mimetic finite difference to compute second order regularization, would provide the best results, with an enlarged dynamic range.

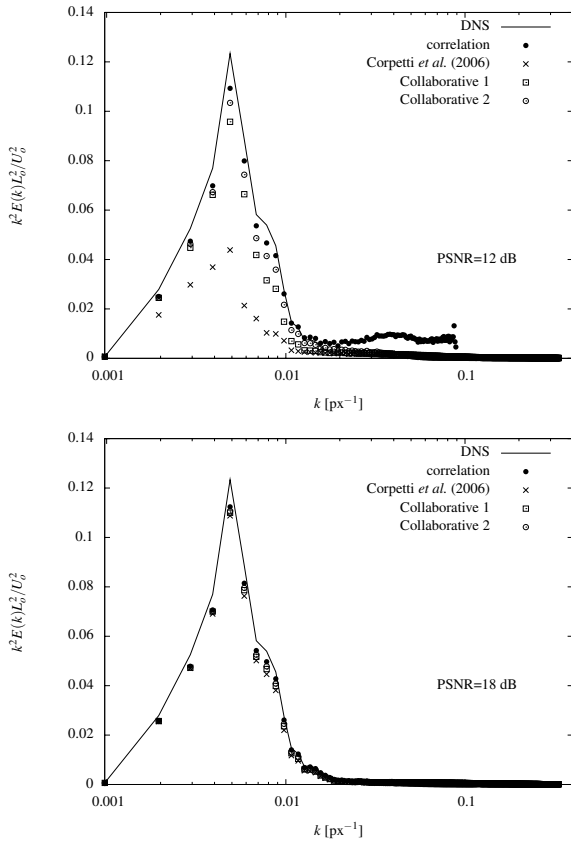


Fig. 4 Compensated energy spectra (linear vertical scale).

### 4.3 Collaborative approach

As shown in figure 2 the collaborative approach resulted in lower RMS error. The proposed technique allowed the estimation of the large displacements with a deviation from the exact velocity modulus lower than 5% (see Fig. 6). In addition collaborative 2 scheme provided an enlargement of the extracted dynamic range. This improvement that could be gained with the proposed approach is shown in figure 5, for wave number around 0.2 pixels for PSNR=12 dB (i.e. wavelength around 50 pixels), and between 0.04 and 0.07 pixels for PSNR=24 dB (i.e. for wavelength between 25 and 14 pixels). The results is quite successful. The collaborative approach provided a robust over noise and dense estimations.

While considering the RMS of the error and with decreasing noise in the images, collaborative 1 approach converged towards optical flow estimation, whereas collaborative 2 approach converged towards correlation estimation. The difference of performance between collaborative 1 and 2 approaches was explained by the influence of the initialization on the minimization of a highly nonlinear problem. Due to its differential nature, the variational formulation of optical flow equations (Eq. 2) relies on the assumption of infinitesimal displacements. To handle large displacements it is common to use the expression in an integrated way (DFD equation). This last form, valid whatever the mangi-

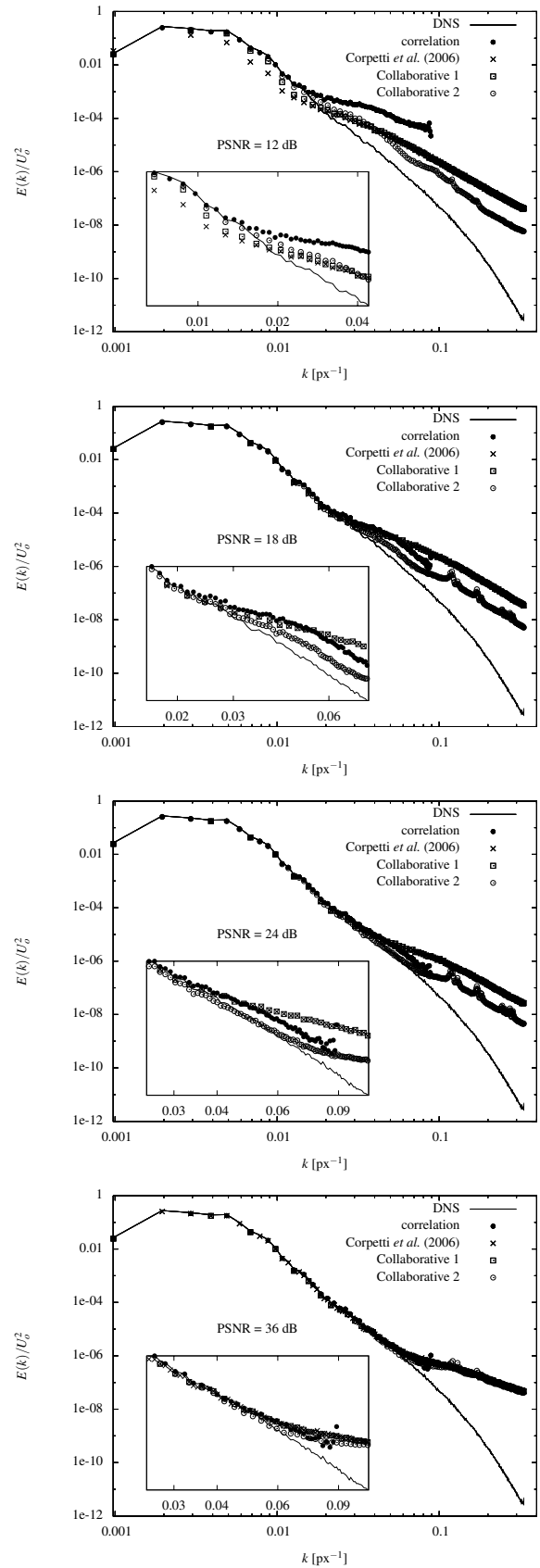


Fig. 5 Comparisons of energy spectra for different approaches and different signal to noise ratios.

tude of the displacement be, is however highly nonlinear in the unknown vector. Hence, most of the time the expression is linearized around a previous estimate and embedded in a multiresolution scheme. In the proposed collaborative approach, the coarse estimates of the multiresolution scheme was replaced by the large displacements  $\bar{\mathbf{u}}$  constrained to be close to a sparse correlation-based vector field  $\mathbf{u}_c$ , the resulting small displacement field  $\mathbf{u}'$ , being supposed to be sufficiently small to satisfy the intrinsic assumption of the variational formulation. However, in practice correlation-based technique acts as a low-pass filtering process with the addition of some errors, depending on the experimental conditions. As a consequence, the resulting field, corresponding to the supposed small displacements  $\mathbf{u}'$  to be estimated, can include some large displacements. In the present turbulent flow considered, since curvature and gradient effects (Hain & Kähler, 2007) associated with noise led to error in the measured vector field, the resulting velocity field included large displacements compared to the assumption of small linear displacements. Furthermore, since the nonlinearity of the minimization problem is high, it needs proper starting values to not get stuck into local minimums and find the global minimum. For collaborative 1 scheme, the vector field  $\mathbf{u}'$  was estimated without any prior knowledge for the starting values. Whereas, for collaborative 2 scheme,  $\mathbf{u}'$  and  $\mathbf{u}$  were estimated at the same time, leading to the estimation of  $\mathbf{d} = \mathbf{u} + \mathbf{u}'$  with the correlation-based vector field  $\mathbf{u}_c$  as initial values. In addition, with collaborative 1 scheme the small scale vector field  $\mathbf{u}'$  was regularized, whereas with collaborative 2 scheme the full vector field  $\mathbf{d}$  was regularized, which provides more accurate estimations.

## 5 Experimental evaluation

The collaborative approach was also applied to a PIV image sequence recorded in one of the wind tunnels of the Rennes regional Center of the Cemagref. The sequence shows the near wake flow of a circular cylinder at Reynolds number  $Re = 3900$ .

The circular cylinder had a length  $L = 280$  mm and a diameter  $D = 12$  mm. It was equipped with two thin rectangular end plates with the specification recommended by Stansby (1974). The distance between the end-plates was 240 mm providing an aspect ratio  $L/D = 20$ . The blockage ratio was 4.3%. The circular cylinder was mounted horizontally at  $3.5D$  from the entrance of the testing zone. The free-stream velocity was adjusted at  $4.8 \text{ m} \cdot \text{s}^{-1}$ .

2D2C PIV experiments were carried out with a LaVision commercial system including a NewWave laser Solo 3 Nd-YAG (Energy by pulse of 50 mJ) and 2 PCO cameras SensiCam (CCD size of  $1280 \times 1024 \text{ px}^2$ , pixel size of  $6,7 \times 6,7 \mu\text{m}^2$  and dynamics of 12 bits). The diameter of the particle seeding (diluted polyglycol in water) were less than  $10 \mu\text{m}$  leading observed diameters around 1-2 pixels size. A Lens with focal length of 50 mm and aperture of 5.6 was mounted on the camera. The field of view was  $3,6D \times 2,9D$ .

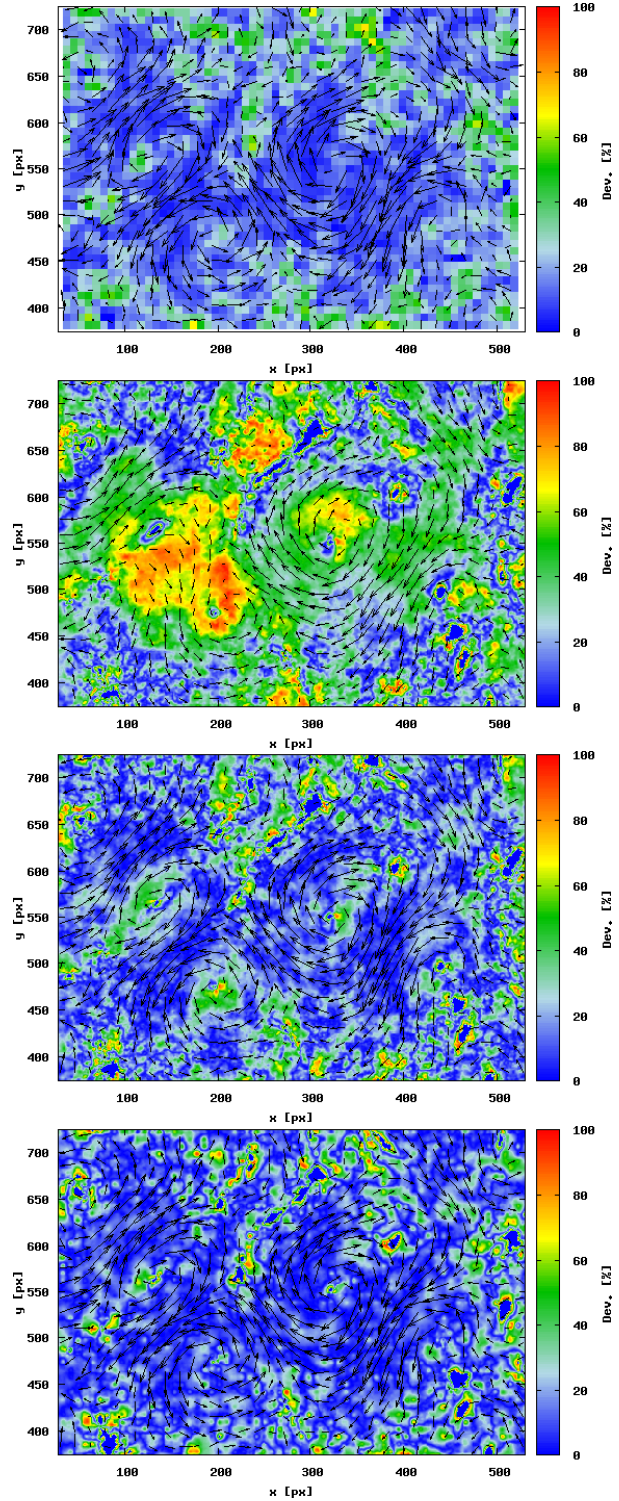


**Fig. 6** Deviation of different approaches from the exact velocity modulus and corresponding vector field – From top to bottom: correlation, optical-flow from Corpetti *et al.* (2006), collaborative 1, collaborative 2. PSNR = 12 dB.

The correlation-based velocity fields were calculated with the commercial software DaVis 6.2 from LaVision. A multipass algorithm with a final interrogation window size of  $16 \times 16 \text{ px}^2$  and 50% overlapping was applied. Image deformation and round gaussian weighing function were used. Spurious velocities were identified with median filter and replaced by the median.

Figure 7 shows the estimated velocity fields using optical flow technique (Corpetti *et al.*, 2006) and the proposed collaborative 2 approach. Optical flow method under-estimated the external high velocity which was approximately two times smaller than the ground truth. This large error was reduced significantly by using the proposed collaborative approach. In figure 8, the vorticity color map of correlation-based and collaborative approaches are shown. Less noisy vorticity map were provided by the collaborative scheme, associated with a finer description of the flow. This evaluation with experimental data indicated that the proposed collaborative approach yielded reliable results where classical optical flow techniques failed, with enlargement towards small scales of the spatial description compared to correlation-based technique.

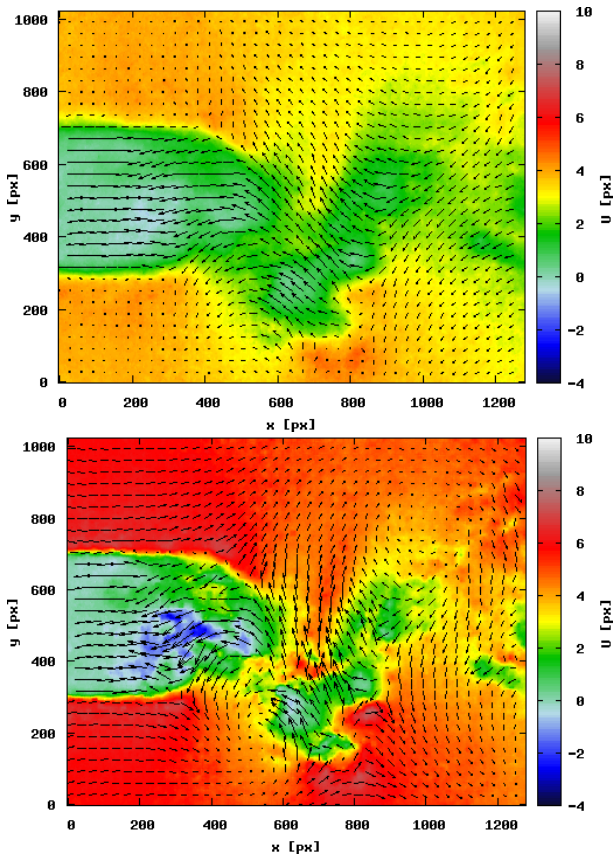


**Fig. 7** Instantaneous vector field with horizontal velocity color map, in near the wake of a circular cylinder at  $Re = 3900$ . Top, optical-flow approach (Corpetti *et al.*, 2006); Bottom, proposed collaborative approach.

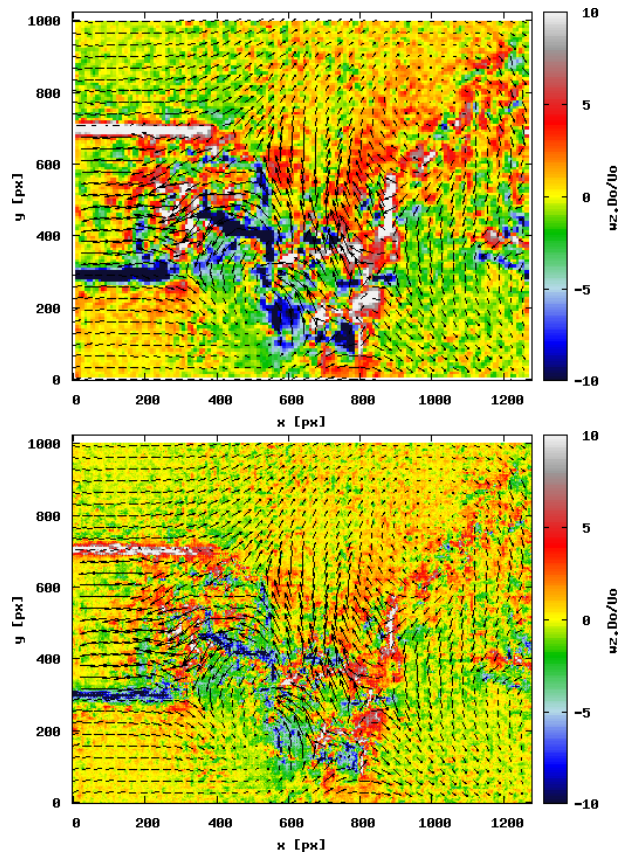


**Fig. 8** Instantaneous vector field with vorticity color map, in near the wake of a circular cylinder at  $Re = 3900$ . Top, correlation approach; Bottom, proposed collaborative approach.

## 6 Conclusion

In this paper, we have proposed and evaluated a new method for robust and dense estimations of instantaneous velocities of fluid flows from image sequences. This method is a collaborative approach mixing fluid dedicated optical-flow method with correlation technique. The novel scheme has been specifically designed to provide robust over noise and dense estimations.

The developed approach has been tested on synthetic particle images based on 2D turbulence and on real image sequence recorded in the wake of a circular cylinder. In each cases, we compared our results with the ones issued from PIV and optic-flow. It was pointed out that the collaborative scheme reinforced fluid dedicated optical-flow methods towards robustness, while enlarging the range of scale that can be resolved with correlation-based techniques.

## References

- BERGEN, J., ANADAN, P., ANNA, K. & HINGORANI, R. 1992 Hierarchical model-based motion estimation. In



- Proc. Europ. conf. Computer Vision* (ed. G. Sandini), pp. 237–252. Springer-Verlag.
- BERTERO, M., POGGIO, T. & TORRE, V. 1988 Ill-posed problems in early vision. *Proceedings of the IEEE* **76** (8), 869–889.
- BIGÜN, J. & GRANLUND, G. 1988 Optical flow based on the inertia matrix in the frequency domain. In *Proc. SSAB Symposium on Picture Processing*. Lund, Sweden.
- BLACK, M. & ANANDAN, P. 1996 The robust estimation of multiple motions: Parametric and piecewise-smooth flow fields. *Computer Vision and Image Understanding* **63** (1), 75–104.
- BRUHN, A., WEICKERT, J. & SCHNÖRR, C. 2005 Lucas/Kanade meets Horn/Schunck: combining local and global optic flow methods. *International Journal of Computer Vision* **63** (3), 211–231.
- CARLIER, J. & WIENEKE, B. 2005 Report 1 on production and diffusion of fluid mechanics images and data, Fluid project deliverable 1.2. European Project 'Fluid image analysis and description' (FLUID) – <http://www.fluid.irisa.fr/>.
- CORPETTI, T., HEITZ, D., ARROYO, G., MÉMIN, E. & SANTA-CRUZ, A. 2006 Fluid experimental flow estimation based on an Optical-flow scheme. *Exp. in Fluids* **40**, 80–97.
- CORPETTI, T., MÉMIN, E. & PÉREZ, P. 2002 Dense estimation of fluid flows. *IEEE Trans on Pattern Analysis and Machine Intelligence* **24** (3), 365–380.
- HAIN, R. & KÄHLER, C. 2007 Fundamentals of multiframe particle image velocimetry (PIV). *Exp Fluids* **42**, 575–587.
- HEITZ, D., NAVAZA, V. & CARLIER, J. 2006 Intermediate report on the evaluation of the tasks of the workpackage 2, Fluid project deliverable 5.1. European Project 'Fluid image analysis and description' (FLUID) – <http://www.fluid.irisa.fr/>.
- HORN, B. & SCHUNCK, B. 1981 Determining optical flow. *Artificial Intelligence* **17**, 185–203.
- LECORDIER, B. & WESTERWEEL, J. 2003 The EUROPIV Synthetic Image Generator (SIG). In *Particle image velocimetry: recent improvements* (ed. M. Stanislas, J. Westerweel & J. Kompenhans), pp. 145–162. EUROPIV 2 workshop, Springer.
- LUCAS, B. & KANADE, T. 1981 An iterative image registration technique with application to stereo vision. In *Proc. Seventh International Joint Conference on Artificial Intelligence*, pp. 674–679. Vancouver, Canada.
- MÉMIN, E. & PÉREZ, P. 2002 Hierarchical estimation and segmentation of dense motion fields. *Int. J. Computer Vision* **46** (2), 129–155.
- RUHNAU, P., KOHLBERGER, T., SCHNÖRR, C. & NOBACH, H. 2005 Variational optical flow estimation for particle image velocimetry. *Exp. in Fluids* **38**, 21–32.
- STANSBY, P. K. 1974 The effects of end plates on the base pressure coefficient of a circular cylinder. *Aeronautical Journal* **78**, 36–37.
- SUTER, D. 1994 Motion estimation and vector splines. In *Proc. Conf. Comp. Vision Pattern Rec.*, pp. 939–942. Seattle, USA.
- YUAN, J., SCHNÖRR, C. & STEIDL, G. 2007 Simultaneous higher-order optical flow estimation and decomposition. *SIAM J. Sci. Computing*, in press.